Published in final edited form as:
Exp Neurol. 2008 April ; 210(2): 750–761. doi:10.1016/j.expneurol.2008.01.012.

Chronic administration of morphine is associated with a decrease in surface AMPA GluR1 receptor subunit in dopamine D1 receptor expressing neurons in the shell and non-D1 receptor expressing neurons in the core of the rat nucleus accumbens

Michael J. Glass[1,*], **Diane A. Lane**[1], **Eric E.O. Colago**[1], **June Chan**[1], **Stefan D. Schlussman**[2], **Yan Zhou**[2], **Mary Jeanne Kreek**[2], and **M. Pickel Virginia**[1]

[1] Department of Neurology and Neuroscience, Well Medical College of Cornell University, NY 10021

[2] Laboratory of the Biology of Addictive Diseases, The Rockefeller University, NY, NY 10021

Abstract

The nucleus accumbens (Acb) is an extensively studied neuroanatomical substrate of opiate reward and the neural plasticity associated with chronic opioid use. The cellular mechanisms mediating opioid-dependent plasticity are uncertain, however AMPA-type glutamate receptor trafficking in dopamine D1 dopamine receptor (D1R) expressing neurons may be a potential cellular pathway for these adaptations, although there is no evidence for this possibility. Immunogold electron microscopy was used to quantify the surface expression of the AMPA GluR1 subunit in dendritic profiles of neurons in the Acb in response to intermittent 14-day non-contingent injections of escalating doses of morphine, a model that parallels opioid self-administration. To determine if changes in GluR1 trafficking occurred in neurons potentially sensitive to dopamine-induced D1R activation, immunoperoxidase labeling of D1R was combined with immunogold labeling of GluR1. Immunogold quantification was performed in two distinct Acb subregions, the shell, an area involved in processing incentive salience related to rewarding stimuli, and the core, an area involved in reward-seeking behaviors. We provide the first report that chronic morphine administration is associated with a receptor-phenotypic decrease in surface trafficking of GluR1 in Acb subregions. When compared to saline injected animals, morphine produced a decrease in plasma membrane GluR1 labeling in medium- and large-size D1R expressing dendritic profiles in the Acb shell. In contrast, in the Acb core, surface GluR1 was decreased in small-size dendrites that did not express the dopamine receptor. These results indicate that chronic intermittent injection of escalating doses of morphine is accompanied by ultrastructural plasticity of GluR1 in neurons that are responsive to glutamate and dopamine-induced D1R activation in the Acb shell, and neurons capable of responding to glutamate but not D1R receptor stimulation in the Acb core. Thus, AMPA receptor trafficking associated with chronic opiate exposure in functionally distinct areas of the Acb may be distinguished by D1R receptor activation, suggesting the potential for differing neural substrates of reward and motor aspects of addictive processes involving glutamate and dopamine signaling.

*Correspondence to: Dr. Michael J. Glass, Department of Neurology and Neuroscience, 411 E. 69th St, Well Medical College of Cornell University, NY, NY 10021.

Keywords

Addiction; Dopamine; Dopamine D1R receptor; Nucleus accumbens core; Nucleus Accumbens shell; Glutamate; Synaptic Plasticity

INTRODUCTION

The nucleus accumbens (Acb), a "limbic-motor interface" (Mogenson 1987) within the ventral striatum, is an extensively studied neuroanatomical substrate of both the affective and behavioral properties of natural and pharmacological reward (Kelley and Berridge 2002; Volkow and Wise 2005). The Acb may also be an important site of neural plasticity associated with chronic use of abused substances, including opioids (Self 2004). However, the cellular mechanisms subserving opioid-dependent adaptations in limbic and motor components of the Acb are largely unknown.

The μ-opioid receptor (μOR) plays an essential role in the rewarding efficacy of morphine, and in the neural and behavioral adaptations associated with chronic opioid exposure, including tolerance and dependence (Chefer et al. 2003; Matthes et al. 1996). Therefore, changes in μOR expression or signal transduction pathways in the Acb may play key roles in the cellular plasticity induced by chronic opioid exposure. However, while μOR mRNA, protein, and ligand binding sites are enriched within the Acb (Mansour et al. 1994; Moriwaki et al. 1996), chronic morphine exposure does not appear to produce obvious signs of μOR plasticity in this brain region (Buzas et al. 1996; Maher et al. 2005; Noble and Cox 1996).

Coordinated communication between glutamatergic and dopaminergic systems in the Acb is emerging as a critical signaling complex associated with reward and neural plasticity accompanying reward-related learning (Hernandez et al. 2005), processes associated with opioid exposure. Thus, indirect effects of μOR stimulation on glutamatergic and dopaminergic signaling may form an alternative framework for conceptualizing the mechanisms of opioid-dependent plasticity in the Acb. In accordance with this idea, the Acb is a major site of integration of glutamatergic and dopamine afferents. The Acb receives a robust glutamatergic input from the basolateral amygdala (BLA), ventral subiculum, and prefrontal cortex (PFC). In addition, the Acb also receives a major projection from ventral tegmental area (VTA) afferents containing the catecholamine neuromodulator dopamine (French and Totterdell 2004; Gerfen et al. 1987; Kalivas and Volkow 2005). Nucleus accumbens glutamate and dopamine influence reward through actions on the ionotropic AMPA-type glutamate and the G-protein-coupled D1R receptors, respectively (Kelz et al. 1999; Layer et al. 1993; Shippenberg et al. 1993).

Repeated use of addictive drugs may contribute to adaptations in glutamate signaling in the Acb (Kalivas and Volkow 2005). As with other forms of experience-dependent plasticity (Malenka 2003), AMPA receptor trafficking may be an important cellular correlate of chronic opiate exposure (Glass et al. 2005). Indeed, it has been shown that long-term depression (LTD) in the Acb is associated with an increase in AMPA receptor internalization, a process that may be involved in addictive behavior (Brebner et al. 2005). There is also evidence that D1R receptor activation may play an important role in AMPA receptor trafficking (Mangiavacchi and Wolf 2004), particularly involving the GluR1 subunit, which, in the absence of GluR2, renders AMPA receptors permeable to calcium (Cull-Candy et al. 2006). However, there is no evidence that chronic administration of escalating doses of morphine can affect the subcellular location of GluR1 containing AMPA receptors in D1R expressing neurons in the Acb.

A critical feature of the Acb is its high degree of organizational and functional specialization (Zahm 2000). There are two generally recognized divisions of the Acb, the shell and core (Brog et al. 1993; Heimer et al. 1991; Kelley 2004). The Acb shell is innervated by a diverse array of afferents including integrative cerebral cortical, amygdala, and hippocampal inputs, as well as thalamic-hypothalamic and midbrain regions (Zahm 2000). Along with other subdivisions of the extended amygdala, the Acb shell is critically involved in integrative functions associated with the experience of motivationally salient stimuli, processes involving glutamate and dopamine signaling (Kelley 2004). The Acb core receives a less diverse compliment of inputs from the cerebral cortex, palladium, amygdala, thalamus, and midbrain (Zahm 2000). The Acb core is an important part of sensory-motor circuitry that mediates reward seeking behavior, a process that involves glutamatergic anterior cingulate and orbitofrontal cortical afferents (Kalivas and Volkow 2005). In conjunction with the functional specialization of the Acb shell and core, local dopamine release may be differentially engaged by motivational events in each region, with a generally greater involvement of the shell in response to primary rewarding or aversive stimuli (Deutch and Cameron 1992; Pontieri et al. 1995; Sokolowski et al. 1998). However, there is no evidence that chronic morphine exposure is exclusively associated with GluR1 trafficking in D1R receptor containing neurons in these regions.

Immunogold electron microscopy has the spatial resolution necessary for the detection of protein immunolabeling at distinct subcellular localizations, and is also compatible with dual immunoperoxidase staining for related antigens (Glass et al. 2005; Glass et al. 2004). This approach was used to quantify the subcellular distribution of GluR1 in dendritic profiles of neurons from the Acb shell and core in response to non-contingent morphine injection. To determine if changes in GluR1 trafficking occur selectively in neurons potentially responsive to dopamine stimulation by D1R activation in the Acb shell relative to the core, immunogold labeling of GluR1 was combined with immunoperoxidase detection of the D1R receptor in each subregion. In order to model the daily intermittent exposure and dose escalation that characterize opioid self-administration without the inter-animal variability that can impair between-group comparisons, animals were given non-contingent injections of morphine in escalating doses. The specific dosing regimen was based on mean daily morphine consumption in rats allowed to self-administer escalating doses of morphine over a 14-day period (Glass et al. 2005; Glass et al. 2004), which has also been shown to produce neural adaptations in glutamate receptor localization.

METHODS

Animals

Male Sprague-Dawley rats (250–300 grams; Charles River, Kingston NY) were used in these experiments, which conform to NIH and the respective institutional guidelines for the Care and Use of Laboratory Animals at the Weill Medical College and Rockefeller University. The animals were housed individually in a stress-minimized facility and maintained on a reverse 12-h light-dark cycle, with unlimited access to food and water. All efforts were made to minimize the number of animals used and their suffering.

Drugs and injection schedule

Morphine sulfate (Sigma, St. Louis, MO) was prepared in saline solution, and given intraperitoneally in three daily injections over a 14-day period. The initial daily morphine dose was 18.9 mg/kg/day and reached 69 mg/kg/day at day 14. This dose regimen paralleled average daily consumption in rats allowed to self-administer morphine, as previously reported (Glass et al. 2005; Glass et al. 2004). One hour following the last injection on day 14, the morphine (n=11) and saline (n=11) rats were either used for: (1) immunolabeling (saline: n=8; morphine:

n=8), or (2) collection of blood samples to assess levels of adrenocorticotropic hormone (ACTH) and corticosterone (saline: n=3; morphine: n=3).

Tissue preparation

Rats were anesthetized with sodium pentobarbital (150 mg/kg, i.p.), and their brains were fixed by aortic arch perfusion sequentially with: (a) 15 ml of normal saline (0.9%) containing 1000 units/ml of heparin, (b) 50 ml of 3.75% acrolein in 2% paraformaldehyde in 0.1 M phosphate buffer (PB, pH 7.4), and (c) 200 ml of 2% paraformaldehyde in PB, all delivered at a flow rate of 100 ml/minute. The brains were removed and post-fixed for 30 minutes in 2% paraformaldehyde in PB. A vibrating microtome was used to cut coronal sections 40 μm thick through the forebrain region containing the Acb, as defined by the rat brain atlas of Paxinos and Watson (1986). Tissue sections were next treated with 1.0% sodium borohydride in PB and then washed in PB. Sections then were immersed in a cryoprotectant solution (25% sucrose and 2.5% glycerol in 0.05 M PB) for 15 minutes. To enhance tissue permeability, sections were then freeze-thawed in liquid Freon and liquid nitrogen. Sections were next rinsed in 0.1 M Tris-buffered saline (TS, pH 7.6) and then incubated for 30 minutes in 0.1% bovine serum albumin (BSA) to minimize nonspecific labeling. Rostrocaudally matched pairs of sections from experimental and control animals were simultaneously processed for immunogold-silver and peroxidase dual labeling of GluR1 and D1R, respectively.

Antisera

Rabbit polyclonal antiserum against GluR1 was obtained commercially (Upstate, Lake Placid, NY). The monoclonal rat anti-D1R antibody was raised against the C-terminus of the human D1R receptor (Clone 1-1-F11 S.E6, Sigma RBI, Saint Louis, MO). Both antisera have been extensively characterized and shown to selectively recognize the antigenic peptides (Glass et al. 2005; Hara and Pickel 2005). The dual labeling protocol is modified from that described by Chan et al., (1990).

Immunocytochemical procedures

For dual detection of immunogold labeling of GluR1 and immunoperoxidase labeling of D1R, sections through the Acb were incubated for 48 hours in a solution containing a mixture of GluR1 (1:100) and D1R (1:500) antisera. After incubation, sections were rinsed in TS and prepared first for peroxidase identification of D1R. Sections were incubated in anti-rat IgG conjugated to biotin, rinsed in TS, and then incubated for 30 minutes in avidin-biotin-peroxidase complex (ABC; 1:100; Vectastain Elite Kit, Vector Laboratories) in TBS. The bound peroxidase was visualized by reaction for 5–6 minutes in 0.2% solution of 3, 3′-diaminobenzidine and 0.003% hydrogen peroxide in TS. Sections were then processed for immunogold labeling. Sections were rinsed in 0.01 M PBS (pH 7.4), and blocked for 10 minutes in 0.5% BSA and 0.1% gelatin in PBS to reduce non-specific binding of gold particles. Sections then were incubated for 2 hours in donkey anti-rabbit IgG conjugated with 1 nm gold particles (1:50, AuroProbeOne, Amersham, Arlington Heights, IL). The sections were rinsed in PBS and incubated for 10 minutes in 2% glutaraldehyde. The bound gold particles were enlarged by a 6 minute silver intensification using an IntenSE-M kit (Amersham, Arlington Heights, IL). There is the possibility that ABC reaction product will be intensified by silver enhancement. In our dual labeling experiments, the primary antisera labeled with a gold secondary was omitted as a control for this possibility (Chan et al. 1990). It should also be pointed out that peroxidase reaction product is typically not particulate, but somewhat diffuse in nature, and thus with careful visual inspection not easily confused with silver- enhanced immunogold.

Ultrastructural analysis

Vibratome sections from the Acb shell and core (Figure. 1) that were used for electron microscopic analysis were thin sectioned on an ultramicrotome, mounted on copper grids, and counterstained with lead citrate and uranyl acetate. Three thin sections from each Acb subregion were analyzed from each animal, resulting in a total of 23,088 μm^2 of sampled tissue. Only sections at the tissue-surface interface were selected for analysis to avoid differences in labeling due to differing penetrance of reagents. The images from thin sections in each treatment group were analyzed in a blind manner on a transmission electron microscope (Tecnai 12 BioTwin, Hillsboro, OR). For the analysis of gold particle distributions, we used an established image analysis procedure (Glass et al., 2005). Since most GluR1 labeling was seen on the plasma membrane or in the cytoplasm of dendritic profiles, these profiles were analyzed to determine the density of the GluR1 gold-silver deposits in the plasmalemmal and cytoplasmic compartments. A dendritic profile was considered to be positively labeled for GluR1 when it contained a single gold particle, provided that comparable areas of neuropil contained epon, myelin or other non-GuR1 expressing structures that were devoid of gold-silver deposits. The potential for false positive labeling is likely to be minor because of the following two reasons: (1) immunogold-particles are almost exclusively seen in dendritic profiles, and (2) the number of dendritic profiles containing one or more particles is quite similar to the number that show GluR1 labeling using the more sensitive immunoperoxidase method. In contrast, there is a marked discrepancy between the large number of dendrites and dendritic spines showing GluR1 immunoperoxidase labeling, and the few that contain more than two gold particles. This suggests that the potential for false positive labeling when using the criterion of one gold particle per profile is considerably less than the potential for false negative labeling when using the criterion of two or more gold particles. Ultimately, the impact of this criterion on the plasmalemmal/cytoplasmic distribution of GluR1 would be expected to equally affect dendrites with or without D1 labeling regardless of the treatment conditions. We also ascertained whether potential changes in the glutamate receptor subunit distributions differentially occurred in dendrites with or without D1R immunoreactivity within a single plane of section. These images were then analyzed to determine: (1) the number of labeled dendritic profiles, and (2) the number of gold-silver particles present in the cytoplasm, or in contact with the plasma membrane. Gold particles in contact with any portion of the surface membrane were considered as plasmalemmal. Morphological parameters, including surface area (perimeter) and cross-sectional area were measured using Microcomputer Imaging Device software (MCID, Imaging Research Inc., Ontario, Canada). The classification of dendrites was based upon descriptions by Peters and co-workers (Peters et al. 1991). Statistical analysis was performed using SPSS software. Data were analyzed by one-way factorial ANOVA, and differences in means were analyzed by Fisher's LSD.

Electron Microscopy

Electron microscopic images were obtained using a digital camera (Advanced Microscopy Techniques) interfaced with a transmission electron microscope. For preparation of figures, images were adjusted for contrast and brightness using Photoshop 6.0 software, and imported into PowerPoint, to assemble images and add lettering. For quantification of cross-sectional area, surface area, as well as minor and major axis length digital images were analyzed with MCID software (Interfocus Imaging Ltd, Cambridge, England).

Radioimmunoassay

At the time of decapitation, blood from each rat was collected in EDTA tubes and placed on ice. Blood was then spun in a refrigerated centrifuge, and plasma was separated and stored at −20 °C for ACTH and corticosterone measurement by radioimmunoassay. Corticosterone levels were assayed by using a rat corticosterone ^{125}I kit (ICN Biomedicals, Costa Mesa, CA).

ACTH immunoreactivity levels were assayed from unextracted plasma by using a ^{125}I kit (Nichols Institute, San Juan Capistrano, CA). All ACTH or corticosterone values were determined in duplicate in a single assay.

RESULTS

Visualization of GluR1 immunogold distribution in dendritic processes with or without D1R immunoperoxidase labeling in the Acb shell of rats injected with saline or morphine

The GluR1 subunit was frequently present in dendritic profiles of Acb shell neurons that also contained D1R immunoreactivity. Labeling for D1R in these dendritic profiles was typically diffusely distributed or aggregated near intracellular organelles and along the plasma membrane (Figure 2A). These profiles were most often small to medium-sized with immunogold-silver deposits for GluR1 present in diverse cytoplasmic compartments, including small vesicular organelles characteristic of endoplasmic reticula. In addition, many GluR1 gold particles were also present on the surface membrane of dendritic spines. In spines, gold-silver deposits for GluR1 were typically present on the extrasynaptic surface membrane (Figure 2B), as well as endomembranous organelles (Figure 2C). Many of these spiny appendages received asymmetric type synapses with (Figure 2B) or without apparent perforations (Figure 2C).

A second population of GluR1 labeled dendritic profiles did not show immunoreactivity for D1R. These dendritic profiles were frequently small to intermediate in size and contacted by one or more unlabeled axon terminal (Figure 3A). In these profiles immunogold particles for GluR1 were found on the extrasynaptic plasma membrane, and near small endomembranous organelles. Dendritic profiles containing exclusively GluR1 labeling were also apposed to dendritic processes expressing immunoperoxidase reaction product for D1R (Figure 3B). Immunogold GluR1 labeling was also present beneath the postsynaptic density in small spiny appendages without D1R receptor labeling (Figure 3C).

Based on visual analysis of electron micrographs of all labeled dendritic profiles from the Acb shell of rats administered saline or morphine, there appeared to be distinct treatment-specific differences in the subcellular localization of GluR1. In saline injected animals, there were many medium-size (see Table 1A for size classification) single and dual labeled dendritic profiles that showed immunogold labeling on the surface membrane (Figure 4A). There were also many instances of medium size single and dual labeled dendritic profiles in the Acb shell of rats injected with morphine (Figure 4B). However, there was a noticeable decrease in the apparent frequency of GluR1 immunogold labeling in association with the plasmalemma in these medium size dendritic processes. Interestingly, the decreased surface membrane GluR1 immunogold labeling seemed to be most evident in those dendritic profiles also expressing D1R immunoperoxidase reaction product.

Quantitative comparison of GluR1 immunolabeling in the Acb shell of saline and morphine injected rats

In order to confirm the qualitative visual inspection indicating differences in GluR1 immunogold distribution in saline and morphine administered rats, further quantitative analysis was performed. A total of 1831 dendritic profiles singly labeled for GluR1, or dually labeled for GluR1 and D1R were counted in the Acb shell. Of all GluR1 labeled dendritic profiles counted in this region, 54% (982/1831) were labeled for GluR1 only, while 46% (849/1831) were dual labeled. To determine if there were quantitative differences in the subcellular localization of GluR1 in rats treated with saline or morphine, the proportion of gold particles associated with the cytoplasm and plasmalemma were compared in GluR1 labeled dendritic profiles without or with D1R immunoreactivity. In order to characterize changes in GluR1

localization in different dendritic compartments of single and dual labeled profiles, cluster analysis was used to separate these profiles into small, medium, and large categories (see Table 1A). These roughly correspond to distal, intermediate, and proximal portions of dendrites in Acb neurons, which are almost exclusively medium in size. By grouping dendrites into equivalent size classes, this analysis also controls for small, though significant differences in cross-sectional (1.3±.03 versus 1.1±.02, p<.0001) and surface (4.5±.05 versus 4.2±.04, p<.0001) areas between saline and morphine treated groups, respectively. There were no significant differences in the number of intracellular gold particles per unit cross-sectional area or surface particles per unit surface area in single GluR1 labeled profiles of any size between treatment groups (Figures 5A–B). In addition there was no difference in the number of intracellular gold particles in dual labeled processes in any class of dendritic profile (Figure 5C). However, in comparison to saline injected animals, those receiving morphine had a significantly lower number of GluR1 immunogold particles on the plasma membrane per unit surface area in D1R expressing medium and large dendritic profiles (Figure 5D).

Visualization of GluR1 immunogold labeling in dendritic profiles with or without D1R immunoreactivity in the Acb core of rats injected with saline or morphine

In the Acb core, GluR1 immunogold labeling was associated with diverse subcellular organelles in single and dual labeled dendritic profiles. Immunogold-silver deposits were present on the surface membrane of dendritic processes also containing diffuse immunoperoxidase reactivity for D1R (Figures 6A–B) as well as the intracellular sites in neurons without visible D1R immunoreactivity (Figure 6A). Immunogold labeling of GluR1 was frequently present in small and intermediate size (see Table 1B for size classification) dendritic profiles in saline-injected rats in single and dual labeled profiles. On visual inspection of labeled profiles in the Acb core from saline and morphine injected rats, there were noticeable qualitative differences in the subcellular localization of GluR1 immunoreactivity between the two groups. GluR1 gold labeling was often seen on the extrasynaptic plasma membrane of dendritic processes without immunoperoxidase labeling for D1R (Figure 7A). There also appeared to be fewer gold particles on the plasma membrane of dendritic profiles without D1R immunolabeling in morphine treated animals (Figure 7B).

Based on visual inspection of all labeled dendritic profiles from the Acb core of saline and morphine treated animals, there appeared to be distinct treatment-specific differences in the ultrastructural distribution of GluR1 immunogold labeling. In both saline and morphine injected animals, there were many instances of small-size single and dual labeled dendritic profiles that showed immunogold labeling on the surface membrane (Figures 7A–B). However, there was also a noticeable decrease in the apparent frequency of GluR1 immunogold labeling in association with the plasmalemma in these small dendritic processes without D1R labeling in morphine-injected rats.

Quantitative comparison of GluR1 immunolabeling in the Acb core in saline and morphine injected rats

Images of 1815 dendritic profiles containing labeling exclusively for GluR1, or co-labeled for the dopamine receptor were captured in the Acb core. Of all GluR1 labeled dendritic profiles counted in the core, 63% (1150/1815) were labeled for GluR1, and 37% (665/1815) were dual labeled. To determine if there were quantitative differences in the subcellular localization of GluR1 in saline and morphine injected rats, the number of gold particles associated with the cytoplasm and plasmalemma were compared in different size dendritic profiles (Table 1B). There were no differences in cross-sectional (1.1±.02 versus 1.1±.02, p=.9) and surface (4.2±.04 versus 4.2±.04, p=.9) areas between saline and morphine treated groups. Comparing saline to morphine treated animals, there was no significant difference in the number of intracellular gold particles (Figures 8A), but there was a significant decrease in GluR1 surface labeling

specifically in small-size single labeled profiles (Figure 8B). In dual labeled dendritic profiles in the Acb core, there were no difference in the number of intracellular or plasma membrane gold particles in any size dendritic profiles (Figures 8C–D).

Measurement of stress hormones in saline and morphine-injected rats

Morphine's effect on hypothalamic-pituitary-adrenal (HPA) axis activation was determined by measuring circulating levels of ACTH and corticosterone 30-minutes following each animal's final saline or morphine injection, respectively. Mean plasma levels of ACTH did not significantly differ in saline and morphine groups (294±57 and 225±106 pg/ml; p=.3). However, relative to the saline treated animals, there was a 3-fold decrease in circulating corticosterone in morphine treated rats (261±84 and 81±17 ng/ml), although this difference fell just below the threshold for statistical significance (p=.052).

DISCUSSION

We provide the first evidence that 14-day non-contingent administration of escalating doses of morphine is associated with a decrease in the surface expression of the AMPA GluR1 receptor subunit in the rat Acb shell and core. Whereas the number of single and dual labeled dendritic profiles was similar in the Acb shell and core, only in the shell was there a decrease in GluR1 in neurons expressing the D1R receptor. These results indicate that morphine-induced ultrastructural plasticty involving AMPA receptors may differentially involve dopamine activation of D1R receptors in organizationally and functionally distinct systems of the Acb.

GluR1 targeting in the Acb shell and core

Immunogold labeling of GluR1 was found in diverse subcellular compartments in dendritic profiles of Acb neurons. GluR1 immunolabeling was present in association with small vesicular organelles characteristic of transport vesicles, as well as tubulovesicular organelles resembling smooth endoplasmic reticula. In addition, GluR1 was also frequently found near the extrasynaptic plasma membrane. Almost half of all GluR1 labeled dendritic processes also showed immunoperoxidase labeling for D1R. In D1R labeled dendritic processes, with or without GluR1 immunogold labeling, immunoperoxidase reaction product was typically present near intracellular organelles and the plasma membrane. Most exclusively GluR1 labeled, as well as dual labeled dendritic processes were small to intermediate in size and were contacted by one or more unlabeled axon terminal, many of which formed asymmetric excitatory-type synapses. While we cannot conclusively identify the source of glutamatergic axons contacting GluR1 expressing dendrites, the particular dendritic compartments where they form excitatory synapses can provide clues regarding their identity. Excitatory afferents arising from the prefrontal cortex tend to contact small dendritic processes, compared to those arising from the BLA, while axon terminals from the ventral subiculum contact even larger dendrites (French and Totterdell 2004). Thus, the decreased surface GluR1 labeling in small Acb core dendritic profiles suggests that these processes are contacted by glutamatergic cortical afferents. In addition, putative dopamine containing axon terminals expressing tyrosine hydroxylase, the rate-limiting enzyme in catecholamine synthesis (Zigmond et al. 1989), also innervate distal dendrites of Acb core neurons (Meredith 1999). More proximal Acb shell dendrites showing changes in surface GluR1 may be contacted by afferents from the subiculum (French and Totterdell 2004), as well as TH-expressing terminals, which are also known to have robust contacts with proximal dendrites of Acb shell neurons (Meredith 1999).

GluR1 targeting in neurons containing D1R in the Acb shell in response to chronic morphine

Compared to animals receiving saline, rats injected with morphine showed a significant reduction of GluR1 immunogold particles on the dendritic plasmalemma of D1R expressing Acb shell neurons. Previous electron microscopic immunolabeling analyses of Acb shell

neurons have also shown that the dendritic plasma membrane, a presumptive functional site for activation of AMPA and many other receptors, is also enriched in μOR (Svingos et al. 1996) and the D1R (Hara et al. 2006). Together, these findings suggest that intracellular signaling cascades that link opioid stimulation, dopamine-mediated D1R activation, and AMPA trafficking may play important roles in the effects of morphine exposure on neural signaling in the Acb. In this regard, it is important to note that morphine administration and withdrawal can profoundly impact dopamine release in the Acb shell (Hirose et al. 2005; Pontieri et al. 1995; Rossetti et al. 1992; Tanda et al. 1997). In addition, D1R stimulation can modulate GluR1 phosphorylation (Chartoff et al. 2006) and trafficking (Mangiavacchi and Wolf 2004). A critical part of the pathway linking opioid and D1R activity with AMPA receptor targeting in the Acb shell may involve changes in the activity of protein kinases, such as cAMP-dependent protein kinase (PKA), which regulate GluR1 trafficking (Wang et al. 2005). Thus, it is significant to note that chronic morphine application in primary cultures of GABAergic spiny striatal neurons enhances D1R mediated increases in cAMP levels (Schoffelmeer et al. 1995), and that opioid self-administration is associated with an increase in PKA immunoreactivity in Acb (Self et al. 1995).

GluR1 targeting in neurons without D1R in the Acb core in response to chronic morphine

As was the case in the Acb shell, there was a lower density of GluR1 on the plasmalemma of dendritic profiles in the Acb core in rats chronically administered morphine relative to saline-treated animals. However, unlike the shell, this difference occurred in processes without D1R labeling. This finding is consistent with prior reports showing contrasting roles of dopamine signaling in the shell and core in rewarding and aversive behavior. For example, there is evidence that dopamine release is preferentially elevated in the shell relative to the core in response to opioid self-administration (Pontieri et al. 1995), food motivated behavior (Sokolowski et al. 1998), and short duration immobilization stress (Deutch and Cameron 1992). However, it has also been shown that behavioral sensitization to morphine is associated with an increase in dopamine release in the Acb core, but a decrease in the shell (Cadoni and Di Chiara 1999). The latter finding is consistent with other reports indicating complex relationships between dopamine release in Acb subdivisions and motivational stimuli (Cheng et al. 2003). This complexity likely reflects, in part, region-specific differences in expression levels and cellular location of not only D1R, but also the D2 dopamine receptor (D2R) coupled to inhibitory G-proteins (Jarvie and Caron 1993). That chronic morphine-induced AMPA receptor trafficking may occur in D2R expressing neurons in the Acb core is an intriguing possibility that will need to be subject to further inquiry.

The present finding that chronic morphine exposure is associated with a decrease in GluR1 immunolabeling in the Acb core is consistent with previous evidence that glutamatergic signaling involving AMPA receptors in this brain area plays important roles in addictive behaviors. Direct Acb administration of an AMPA/kainate receptor antagonist reduces cocaine-seeking behavior (Di Ciano and Everitt 2001), a finding similar to that produced by lesion of the cingulate cortex (Bussey et al. 1997). In addition, inhibition of Acb core glutamate release by acutely inhibiting prefrontal cortical afferents can also prevent stress-induced drug-seeking behavior (McFarland et al. 2004). Together, these results demonstrate that AMPA receptor activation by glutamate released from cerebral cortical afferents may play a significant role in drug-procurement. The decreased surface availability of GluR1 expressing AMPA receptors in response to chronic morphine exposure may thus represent a subcellular substrate of drug-induced alterations in neuronal activity within the Acb core, possibly involving cerebral cortical glutamatergic afferents known to play an important role in addictive behaviors (Kalivas and Volkow 2005).

Stress hormone levels in response to morphine

Given the critical role of stress and stress hormones in addictive behaviors (Koob and Kreek 2007), we investigated the effect of morphine on HPA axis activity by measuring plasma levels of the stress-responsive hormones ACTH and corticosterone. While morphine treated rats had corticosterone levels that were three-fold less than those administered saline, these results fell just below the threshold for statistical significance. The decreasing trend in circulating corticosterone is consistent with the tolerance, or even blunting of corticosterone levels seen with repeated opioid exposure (Buckingham and Cooper 1984; Ignar and Kuhn 1990; Zhou et al. 2006), although it contrasts with the surges that follow acute intermittent morphine administration and morphine withdrawal (Zhou et al. 2006; Zhou et al. 1999).

Acknowledgments

Supported by DA-004600 (VMP), DA-05130 and DA-00049 (MJK), DA-016735 (MJG), and DA-007274

References

Brebner K, Wong TP, Liu L, Liu Y, Campsall P, Gray S, Phelps L, Phillips AG, Wang YT. Nucleus accumbens long-term depression and the expression of behavioral sensitization. Science 2005;310:1340–3. [PubMed: 16311338]

Brog JS, Salyapongse A, Deutch AY, Zahm DS. The patterns of afferent innervation of the core and shell in the “accumbens” part of the rat ventral striatum: immunohistochemical detection of retrogradely transported fluoro-gold. J Comp Neurol 1993;338:255–78. [PubMed: 8308171]

Buckingham JC, Cooper T. Differences in hypothalamo–pituitary–adrenal activity in rats after acute and prolonged treatment with morphine. Neuroendocrinol 1984;38:411–417.

Bussey TJ, Everitt BJ, Robbins TW. Dissociable effects of cingulate and medial frontal cortex lesions on stimulus-reward learning using a novel Pavlovian autoshaping procedure for the rat: implications for the neurobiology of emotion. Behav Neurosci 1997;111:908–919. [PubMed: 9383513]

Buzas B, Rosenberger J, Cox BM. Mu and delta opioid receptor gene expression after chronic treatment with opioid agonist. Neuroreport 1996;7:1505–8. [PubMed: 8856708]

Cadoni C, Di Chiara G. Reciprocal changes in dopamine responsiveness in the nucleus accumbens shell and core and in the dorsal caudate-putamen in rats sensitized to morphine. Neurosci 1999;90:447–55.

Chan J, Aoki C, Pickel VM. Optimization of differential immunogold-silver and peroxidase labeling with maintenance of ultrastructure in brain sections before plastic embedding. J Neurosci Methods 1990;33:113–127. [PubMed: 1977960]

Chartoff EH, Mague SD, Barhight MF, Smith AM, Carlezon WA. Behavioral and molecular effects of dopamine D1 receptor stimulation during naloxone-precipitated morphine withdrawal. J Neurosci 2006;26:6450–7. [PubMed: 16775132]

Chefer VI, Kieffer BL, Shippenberg TS. Basal and morphine-evoked dopaminergic neurotransmission in the nucleus accumbens of MOR- and DOR-knockout mice. Eur J Neurosci 2003;18:1915–22. [PubMed: 14622224]

Cheng JJ, de Bruin JP, Feenstra MG. Dopamine efflux in nucleus accumbens shell and core in response to appetitive classical conditioning. Eur J Neurosci 2003;18:1306–14. [PubMed: 12956729]

Cull-Candy S, Kelly L, Farrant M. Regulation of Ca2+-permeable AMPA receptors: synaptic plasticity and beyond. Curr Opin Neurobiol 2006;16:288–97. [PubMed: 16713244]

Deutch AY, Cameron D. Pharmacological characterization of dopamine systems in the nucleus accumbens core and shell. Neurosci 1992;46:49–56.

Di Ciano P, Everitt BJ. Dissociable effect of antagonism of NMDA and AMPA/KA receptors in the nucleus accumbens core and shell on cocaine-seeking behaviour. Neuropsychopharmacol 2001;25:341–360.

French SJ, Totterdell S. Quantification of morphological differences in boutons from different afferent populations to the nucleus accumbens. Brain Res 2004;1007:167–77. [PubMed: 15064148]

Gerfen CR, Herkenham M, Thibault J. The neostriatal mosaic: II. Patch- and matrix-directed mesostriatal dopaminergic and non-dopaminergic systems. J Neurosci 1987;7:3915–34. [PubMed: 2891799]

Glass MJ, Kruzich PJ, Colago EE, Kreek MJ, Pickel VM. Increased AMPA GluR1 receptor subunit labeling on the plasma membrane of dendrites in the basolateral amygdala of rats self-administering morphine. Synapse 2005;58:1–12. [PubMed: 16037950]

Glass MJ, Kruzich PJ, Kreek M, Pickel VM. Decreased plasma membrane targeting of NMDA-NR1 receptor subunit in dendrites of medial nucleus tractus solitarius neurons in rats self-administering morphine. Synapse 2004;53:191–201. [PubMed: 15266550]

Hara Y, Pickel VM. Overlapping intracellular and differential synaptic distributions of dopamine D1 and glutamate N-methyl-D-aspartate receptors in rat nucleus accumbens. J Comp Neurol 2005;492:442–55. [PubMed: 16228995]

Hara Y, Yakovleva T, Bakalkin G, Pickel VM. Dopamine D1 receptors have subcellular distributions conducive to interactions with prodynorphin in the rat nucleus accumbens shell. Synapse 2006;60:1–19. [PubMed: 16575853]

Heimer L, Zahm DS, Churchill L, Kalivas PW, Wohltmann C. Specificity in the projection patterns of accumbal core and shell in the rat. Neurosci 1991;41:89–125.

Hernandez PJ, Andrzejewski ME, Sadeghian K, Panksepp JB, Kelley AE. AMPA/kainate, NMDA, and dopamine D1 receptor function in the nucleus accumbens core: a context-limited role in the encoding and consolidation of instrumental memory. Learning and Memory 2005;12:285–95. [PubMed: 15930507]

Hirose N, Murakawa K, Takada K, Oi Y, Suzuki T, Nagase H, Cools AR, Koshikawa N. Interactions among mu- and delta-opioid receptors, especially putative delta1- and delta2-opioid receptors, promote dopamine release in the nucleus accumbens. Neurosci 2005;135:213–25.

Ignar DM, Kuhn CM. Effects of specific mu and kappa opiate tolerance and abstinence on hypothalamo-pituitary-adrenal axis secretion in the rat. J Pharmacol Exp Therap 1990;255:1287–95. [PubMed: 2175800]

Jarvie KR, Caron MG. Heterogeneity of dopamine receptors. Adv Neurol 1993;60:325–33. [PubMed: 8380525]

Kalivas PW, Volkow ND. The neural basis of addiction: a pathology of motivation and choice. Am J Psychiatry 2005;162:1403–13. [PubMed: 16055761]

Kelley AE. Ventral striatal control of appetitive motivation: role in ingestive behavior and reward-related learning. Neurosci Biobehav Rev 2004;27:765–76. [PubMed: 15019426]

Kelley AE, Berridge KC. The neuroscience of natural rewards: Relevance to addictive drugs. J Neurosci 2002;22:3306–3311. [PubMed: 11978804]

Kelz MB, Chen J, Carlezon WA, Whisler K, Gilden L, Beckmann AM, Steffen C, Zhang YJ, Marotti L, Self DW, Tkatch T, Baranauskas G, Surmeier DJ, Neve RL, Duman RS, Picciotto MR, Nestler EJ. Expression of the transcription factor deltaFosB in the brain controls sensitivity to cocaine. Nature 1999;401:272–6. [PubMed: 10499584]

Koob GF, Kreek MJ. Stress, dysregulation of drug reward pathways, and the transition to drug dependence. Am J Psychiatry 2007;164:1149 – 1159. [PubMed: 17671276]

Layer RT, Uretsky NJ, Wallace LJ. Effects of the AMPA/kainate receptor antagonist DNQX in the nucleus accumbens on drug-induced conditioned place preference. Brain Res 1993;617

Maher CE, Martin TJ, Childers SR. Mechanisms of mu opioid receptor/G-protein desensitization in brain by chronic heroin administration. Life Sci 2005;77:1140–54. [PubMed: 15890372]

Malenka R. Synaptic plasticity and AMPA receptor trafficking. Annals of the New York Academy of Sciences 2003;1003:1–11. [PubMed: 14684431]

Mangiavacchi S, Wolf ME. D1 dopamine receptor stimulation increases the rate of AMPA receptor insertion onto the surface of cultured nucleus accumbens neurons through a pathway dependent on protein kinase A. J Neurochem 2004;88:1261–71. [PubMed: 15009682]

Mansour A, Fox CA, Thompson RC, Akil H, Watson SJ. mu-Opioid receptor mRNA expression in the rat CNS: comparison to mu-receptor binding. Brain Res 1994;643:245–65. [PubMed: 8032920]

Matthes HWD, Maldonado R, Simonin F, Valverde O, Slowe S, Kitchen I, Befort K, Dierich A, Le Meur M, Dolle P, Tzavara E, Hanoune J, Roques BP, Kieffer BL. Loss of morphine-induced analgesia,

reward effect and withdrawal symptoms in mice lacking the mu-opioid-receptor gene. Nature 1996;383:819–823. [PubMed: 8893006]

McFarland K, Davidge SB, Lapish CC, Kalivas PW. Limbic and motor circuitry underlying footshock-induced reinstatement of cocaine-seeking behavior. J Neurosci 2004;24:1551–60. [PubMed: 14973230]

Meredith GE. The synaptic framework for chemical signaling in nucleus accumbens. Annals of the New York Academy of Sciences 1999;877:140–56. [PubMed: 10415648]

Mogenson GJ. Limbic-motor integration. Prog Physiol Psychol 1987;12:117–170.

Moriwaki A, Wang JB, Svingos A, van Bockstaele E, Cheng P, Pickel V, Uhl GR. mu Opiate receptor immunoreactivity in rat central nervous system. Neurochem Res 1996;21:1315–31. [PubMed: 8947922]

Noble F, Cox BM. Differential desensitization of mu- and delta- opioid receptors in selected neural pathways following chronic morphine treatment. Br J Pharmacol 1996;117:161–9. [PubMed: 8825358]

Peters, A.; Palay, SL.; Webster, H. The fine structure of the nervous system. Oxford University Press; 1991.

Pontieri FE, Tanda G, Di Chiara G. Intravenous cocaine, morphine, and amphetamine preferentially increase extracellular dopamine in the “shell” as compared with the “core” of the rat nucleus accumbens. PNAS 1995;92:12304–8. [PubMed: 8618890]

Rossetti ZL, Hmaidan Y, Gessa GL. Marked inhibition of mesolimbic dopamine release: a common feature of ethanol, morphine, cocaine and amphetamine abstinence in rats. Eur J Pharmacol 1992;221:227–34. [PubMed: 1426002]

Schoffelmeer AN, De Vries TJ, Vanderschuren LJ, Tjon GH, Nestby P, Wardeh G, Mulder AH. Glucocorticoid receptor activation potentiates the morphine-induced adaptive increase in dopamine D-1 receptor efficacy in gamma-aminobutyric acid neurons of rat striatum/nucleus accumbens. J Pharmacol Exper Therap 1995;274:1154–60. [PubMed: 7562482]

Self DW. Regulation of drug-taking and -seeking behaviors by neuroadaptations in the mesolimbic dopamine system. Neuropharmacol 2004;47(Suppl 1):242–55.

Self DW, McClenahan AW, Beitner-Johnson D, Terwilliger RZ, Nestler EJ. Biochemical adaptations in the mesolimbic dopamine system in response to heroin self-administration. Synapse 1995;21:312–8. [PubMed: 8869161]

Shippenberg TS, Bals-Kubik R, Herz A. Examination of the neurochemical substrates mediating the motivational effects of opioids: role of the mesolimbic dopamine system and D-1 vs. D-2 dopamine receptors. J Pharmacol Exper Therap 1993;265:53–9. [PubMed: 8386244]

Sokolowski JD, Conlan AN, Salamone JD. A microdialysis study of nucleus accumbens core and shell dopamine during operant responding in the rat. Neurosci 1998;86:1001–9.

Svingos AL, Moriwaki A, Wang JB, Uhl GH, Pickel VM. Ultrastructural immunocytochemical localization of mu-opioid receptors in rat nucleus accumbens: extrasynaptic plasmalemmal distribution and association with Leu(5)-enkephalin. J Neurosci 1996;16:4162–4173. [PubMed: 8753878]

Tanda G, Pontieri FE, Di Chiara G. Cannabinoid and heroin activation of mesolimbic dopamine transmission by a common mu1 opioid receptor mechanism. Science 1997;276:2048–50. [PubMed: 9197269]

Volkow ND, Wise RA. How can drug addiction help us understand obesity? Nature Neurosci 2005;8:555–60. [PubMed: 15856062]

Wang JQ, Arora A, Yang L, Parelkar NK, Zhang G, Liu X, Choe ES, Mao L. Phosphorylation of AMPA receptors: mechanisms and synaptic plasticity. Mol Neurobiol 2005;32:237–49. [PubMed: 16385140]

Zahm DS. An integrative neuroanatomical perspective on some subcortical substrates of adaptive responding with emphasis on the nucleus accumbens. Neurosci Biobehav Rev 2000;24:85–105. [PubMed: 10654664]

Zhou Y, Bendor J, Hofmann L, Randesi M, Ho A, Kreek M. Mu opioid receptor and orexin/hypocretin mRNA levels in the lateral hypothalamus and striatum are enhanced by morphine withdrawal. J Endocrinol 2006;191:137–45. [PubMed: 17065397]

Zhou Y, Spangler R, Maggos CE, Wang XM, Han JS, Ho A, Kreek M. Hypothalamic–pituitary–adrenal activity and pro-opiomelanocortin mRNA levels in the hypothalamus and pituitary of the rat are differentially modulated by acute intermittent morphine with or without water restriction stress. J Endocrinol 1999;163:261–267. [PubMed: 10556776]

Zigmond RE, Schwarzschild MA, Rittenhouse AR. Acute regulation of tyrosine hydroxylase by nerve activity and by neurotransmitters via phosphorylation. Annu Rev Neurosci 1989;12:415–461. [PubMed: 2564757]

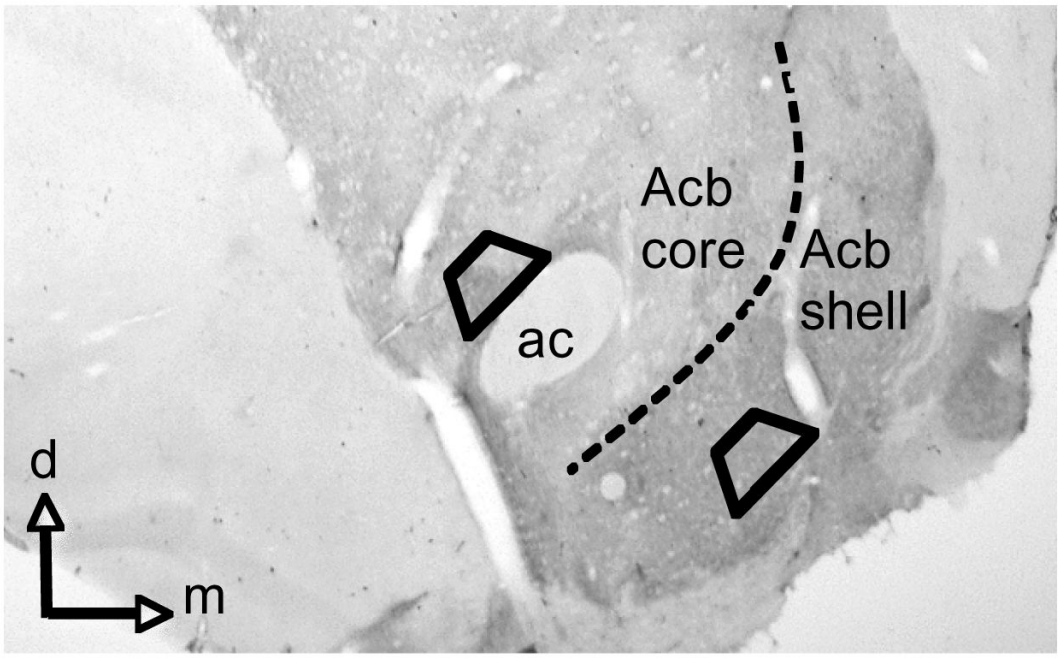

Figure 1.
Light micrograph of brain section processed for dual labeling of GluR1 and D1R that demonstrates Acb subregions. Areas bounded by trapezoids illustrate where thin sections were cut for EM analysis. ac = anterior commissure, d = dorsal, m =medial.

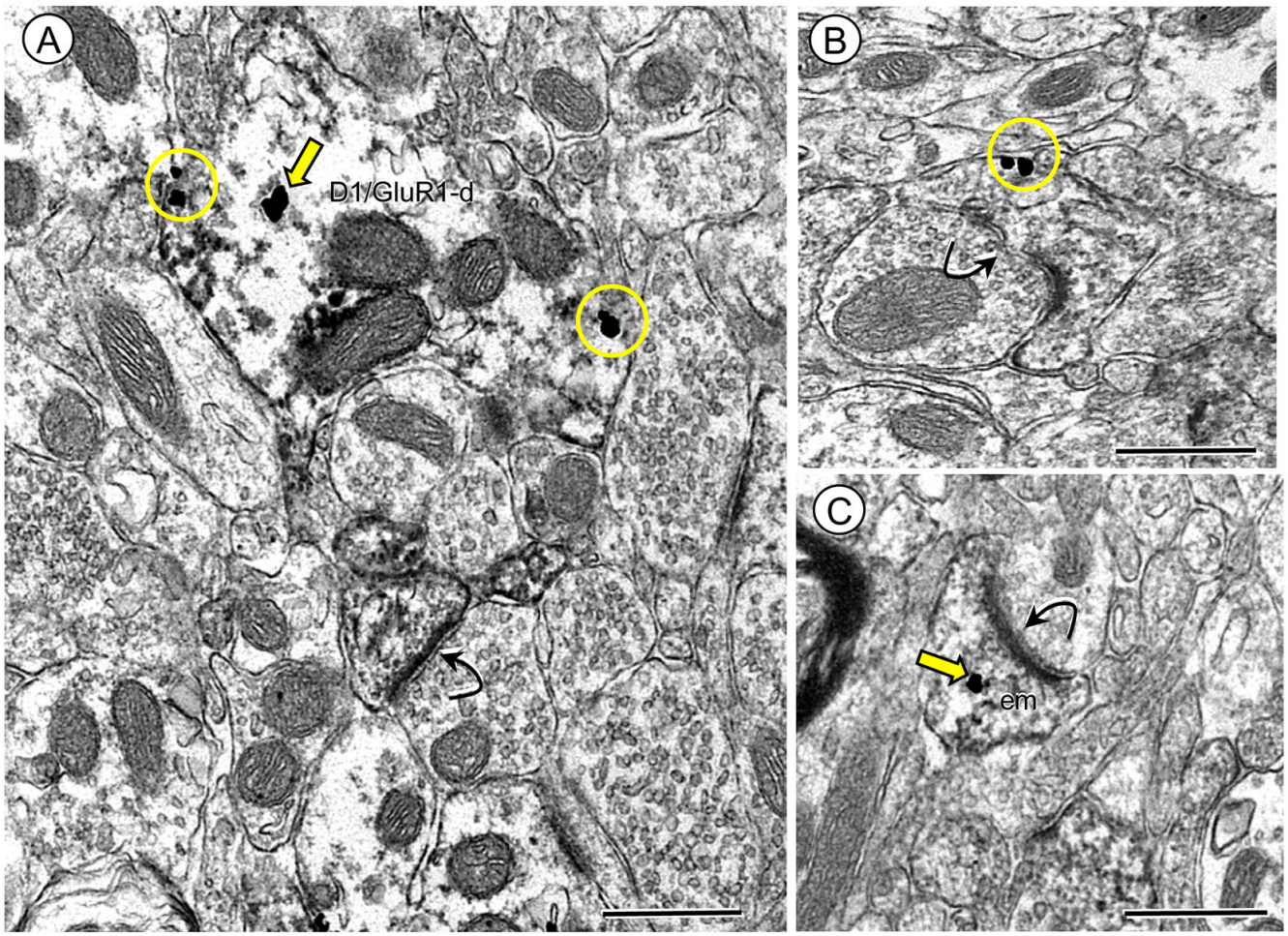

Figure 2.

Immunogold labeling of GluR1 is present at surface and intracellular sites in dendrites also expressing the D1R in Acb shell neurons (A). Electron micrograph shows immunoperoxidase D1R labeling diffusely distributed in a spiny dendrite (D1R/GluR1-d) in which GluR1 immunogold-silver deposits are located intracellularly (arrow) near an endomembrane (em) and on the plasma membrane (circles). (B–C) Dendritic spines receive asymmetric excitatory-type synapses from unlabeled terminals. Spines in B and C show either plasmalemmal (circle) or cytoplasmic (arrow) GluR1 gold labeling, respectively. Scale bars = 0.5 microns.

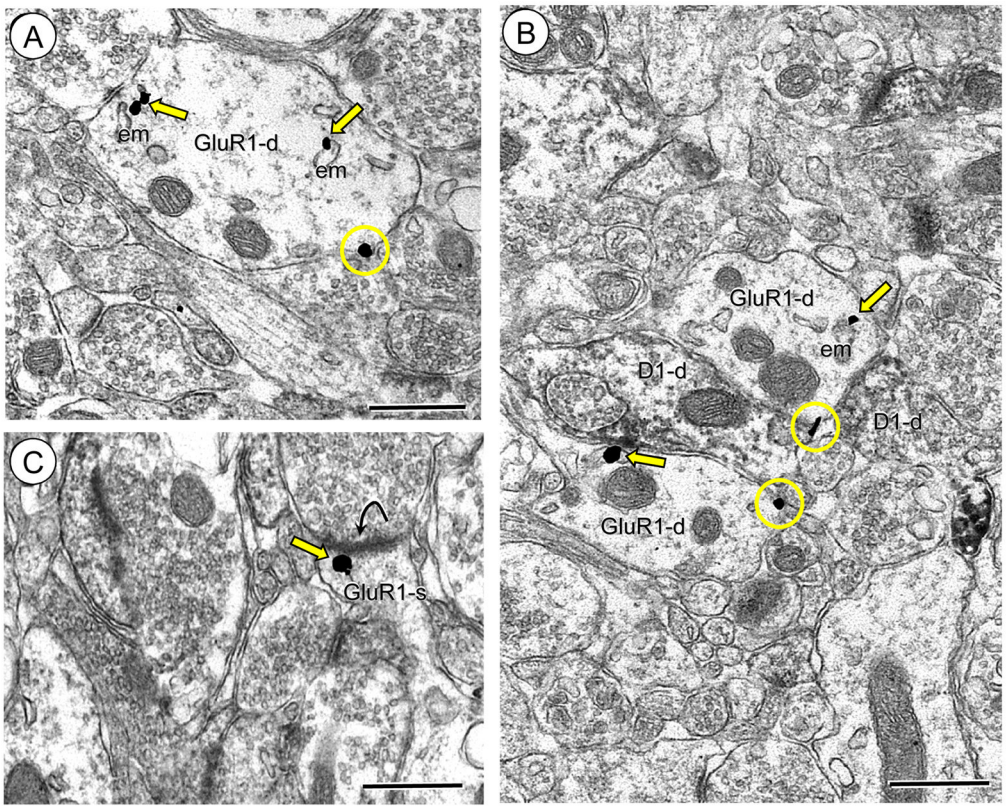

Figure 3.

Immunogold labeling of GluR1 is present at surface and intracellular sites in dendrites without labeling for the D1R in Acb shell neurons. (A). Immunogold labeling for GluR1 is seen on the plasmalemma (circles) or intracellularly (arrows) near an endomembrane (em) in a dendritic profile (GluR1-d). (B). Dendritic profiles exclusively showing GluR1 labeling (GluR1-d) at intracellular and surface sites oppose a dendritic profile only expressing immunoperoxidase reaction product for the D1R (D1R-d). (C). An unlabeled axon terminal forms an excitatory-type synapse (curved arrow) with a dendritic spine (GluR1-s) showing GluR1 gold (arrow) directly beneath the postsynaptic density. Scale bars = 0.5 microns.

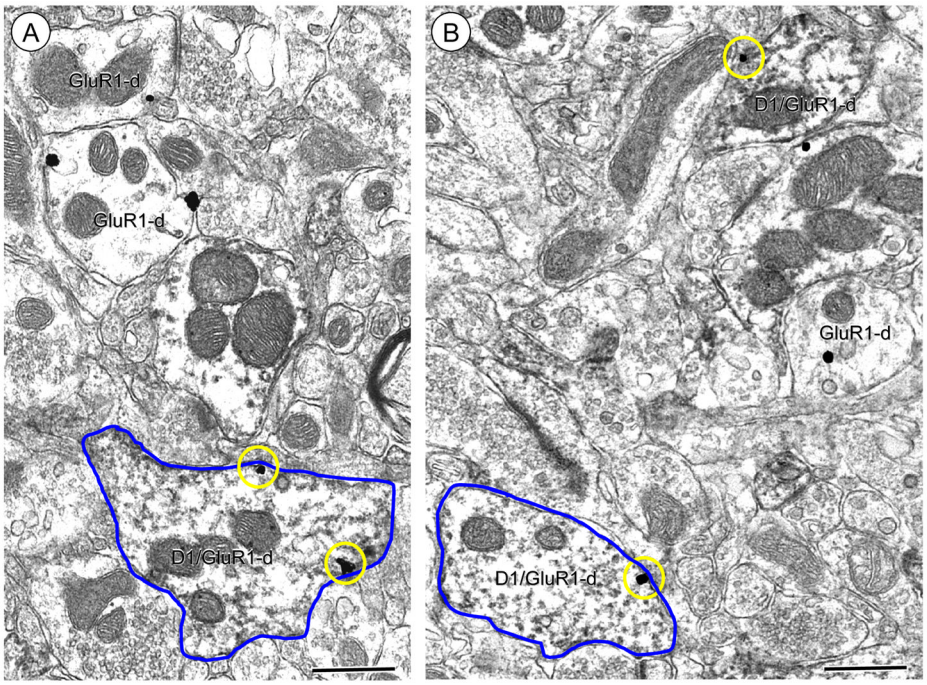

Figure 4.

Immunogold GluR1 labeling in dendritic profiles of neurons from the Acb shell of saline and morphine treated rats. (A–B). Electron micrographs showing more GluR1 immunogold-silver deposits on the plasma membrane of medium-size dendrites containing immunoperoxidase labeling for D1R (D1R/GluR1-d) in rats receiving saline (A) compared with morphine (B). Outlines of representative dendritic profiles are traced in blue. Circles = plasmalemmal GluR1. GluR1-d = GluR1 single label dendrites. Scale bars = 0.5 microns.

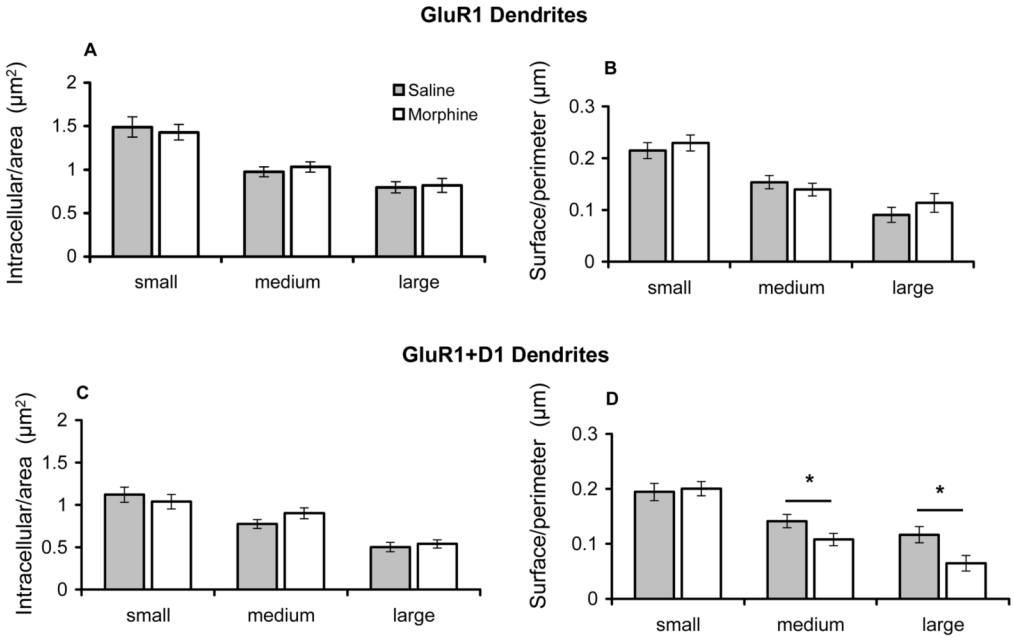

Figure 5.

Bar graphs showing GluR1 distribution in dendritic profiles of neurons from saline and morphine administered rats. (A–B). There are no differences in intracellular or plasmalemmal immunogold labeling in single GluR1 expressing small-, medium- and large-size dendritic profiles in the Acb shell of rats treated with saline or morphine. (C). There is no difference in intracellular GluR1 immunogold labeling in intracellular sites of small-, intermediate-, and large-size profiles in dual labeled dendrites of saline and morphine-treated rats. (D). There is a significant decrease in plasmalemmal GluR1 immunogold labeling in dual labeled medium and large dendritic profiles from the Acb shell of morphine treated rats compared with those administered saline. *$p<0.05$

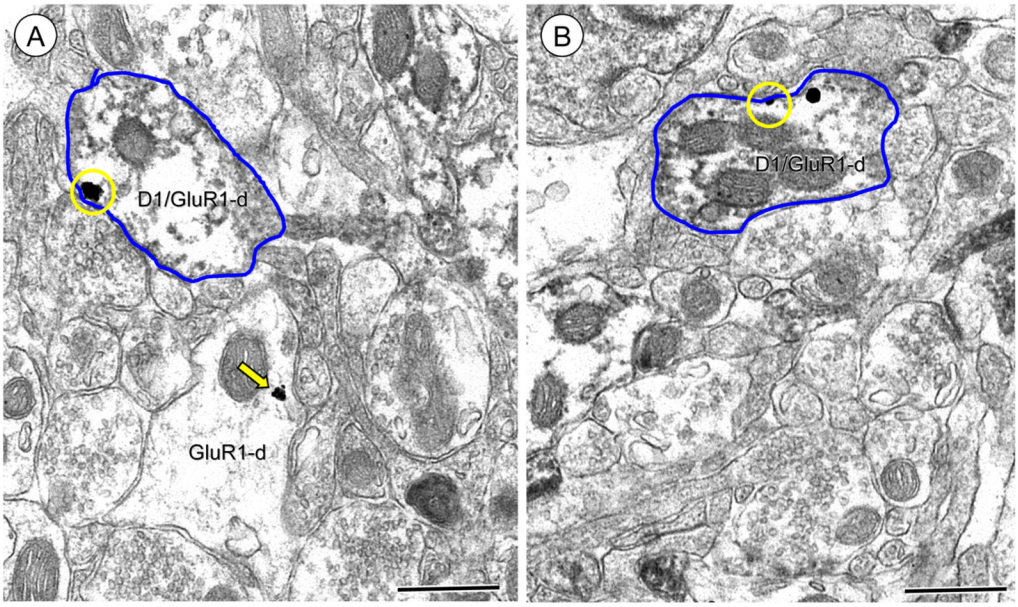

Figure 6.

Immunogold labeling in dual labeled dendritic profiles of Acb core neurons from saline and morphine injected animals. (A–B). Electron micrographs showing no qualitative differences in plasmalemmal (circles) GluR1 immunogold labeling in dendrites containing immunoperoxidase reaction product for D1R receptors (D1R/GluR1-d) in saline (A) and morphine (B) treated rats. GluR1 immunogold (arrow) is also seen in a single labeled dendrite (GluR1-d) in A. Representative dendritic profiles are traced in blue. Scale bars = 0.5 microns.

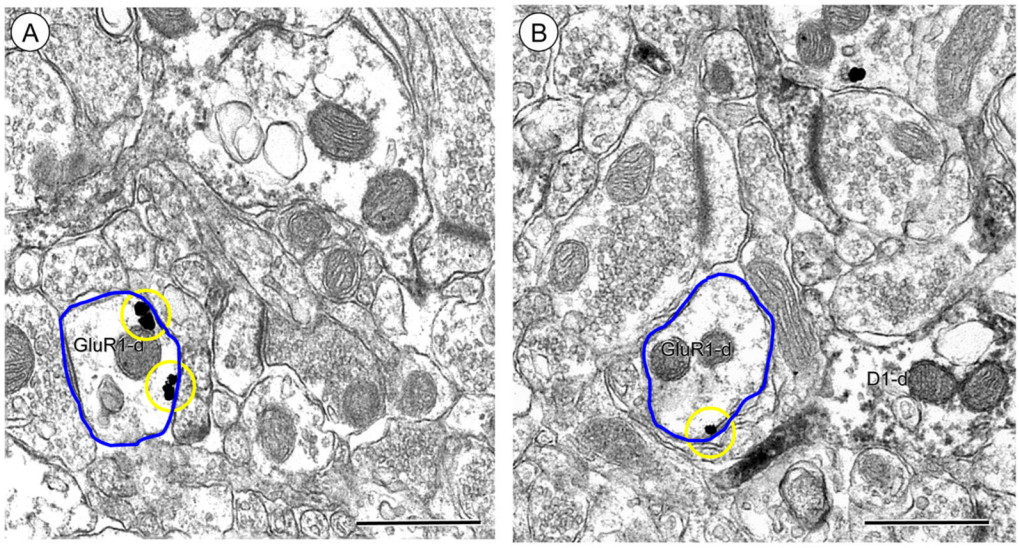

Figure 7.
Immunogold GluR1 expression in single labeled dendritic profiles of Acb core neurons from saline and morphine injected animals. (A–B). Electron micrographs showing qualitatively greater abundance of plasmalemmal (circles) GluR1 immunogold in small dendrites (GluR1-d) from the Acb core of rats receiving saline (A) relative to those treated with morphine (B). Representative dendritic profiles are traced in blue. Scale bars = 0.5 microns.

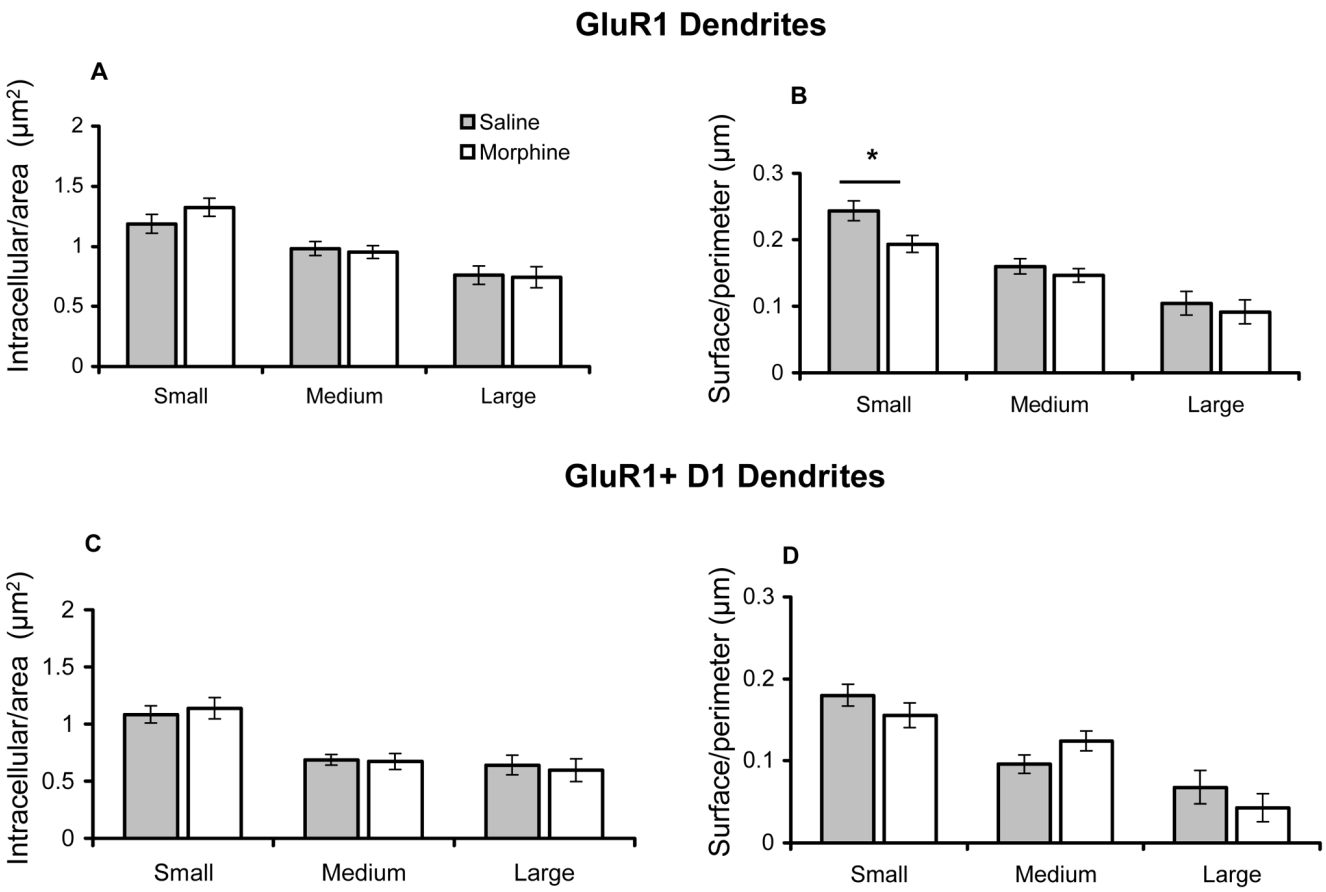

Figure 8.

Bar graphs showing GluR1 distribution in dendritic profiles of neurons from saline and morphine injected rats. (A). There are no differences in intracellular GluR1 immunogold labeling in small, intermediate, or large single labeled dendritic profiles of Acb core neurons in saline or morphine treated rats. (B). There is a selective decrease in surface GluR1 labeling in small single labeled dendritic profiles of Acb core neurons in morphine administered rats, compared with those treated with saline. (C-D). There are no differences in intracellular or plasmalemmal GluR1 immunogold labeling in small, intermediate, or large dendritic profiles of dual labeled Acb core neurons in saline or morphine treated animals. *$p<0.05$

Table 1

Size categories of single and dual labeled dendritic profiles in the Acb shell and core.

A. Cluster analysis of minor axis siz e:					
Area in NA	**Labeling**	**Dendrite size**	**Number of dendrites**	**Minimum (µm)**	**Maximum (µm)**
shell	D1/GluR1	Small	386	.36	.84
		Medium	361	.85	1.25
		Large	102	1.26	2.26
		Total	849		
	GluR1 only	Small	480	.33	.84
		Medium	380	.85	1.25
		Large	122	1.26	2.71
		Total	982		

B. Cluster analysis of minor axis siz e:					
Area in NA	**Labeling**	**Dendrite size**	**Number of dendrites**	**Minimum (µm)**	**Maximum (µm)**
core	D1/GluR1	Small	353	.31	.83
		Medium	270	.84	1.24
		Large	42	1.25	2.45
		Total	665		
	GluR1 only	Small	566	.32	.83
		Medium	481	.84	1.25
		Large	103	1.26	3.43
		Total	1150		